Available online at www.sciencedirect.com
ScienceDirect
Journal of Catalysis 243 (2006) 212–216
JOURNAL OF CATALYSIS
www.elsevier.com/locate/jcat

Research Note

Iron site modification upon alkaline treatment of Fe-ZSM-5 zeolites—Opportunities for improved N_2O decomposition activity

J.C. Groen [a,*], A. Brückner [b], E. Berrier [b], L. Maldonado [c], J.A. Moulijn [a], J. Pérez-Ramírez [c,d]

[a] *DelftChemTech, Delft University of Technology, Julianalaan 136, 2628 BL Delft, The Netherlands*
[b] *Institut für Angewandte Chemie, Berlin-Adlershof, P.O. Box 961156, D-12474 Berlin, Germany*
[c] *Institute of Chemical Research of Catalonia (ICIQ), Av. Països Catalans 16, E-43007 Tarragona, Spain*
[d] *Catalan Institution for Research and Advanced Studies (ICREA), Passeig Lluís Companys 23, E-08010 Barcelona, Spain*

Received 9 May 2006; revised 29 June 2006; accepted 6 July 2006

Available online 22 August 2006

Abstract

Alkaline treatment of Fe-ZSM-5 zeolite induces substantial intracrystalline mesoporosity and enhances the population of isolated Fe^{3+} at the expense of oligonuclear clusters. In situ UV/vis showed that this redispersion affects the redox properties of the alkaline-treated zeolite and leads to lower activity in direct N_2O decomposition compared with the parent sample. Subsequent ion exchange of the alkaline-treated sample in ammonium nitrate solutions induced a renewed alteration in iron speciation, resulting in a similar constitution as in the parent zeolite but with a higher concentration of Fe^{2+} sites able to activate N_2O. Mechanistic investigations in the TAP reactor furthermore affirmed that these newly obtained species had improved oxygen desorption, which correlates with the superior activity in direct N_2O decomposition.

Keywords: Desilication; Post-synthesis modification; Alkaline treatment; Mesopore formation; Fe-ZSM-5; Zeolite; N_2O decomposition; Redox activity

1. Introduction

Iron-containing zeolites have revealed outstanding performance in various catalytic conversions related to environmental applications (e.g., direct N_2O decomposition, selective catalytic reduction of NO_x and N_2O, selective oxidation of NH_3 to N_2) and in oxidative transformations of hydrocarbons (e.g., benzene and phenol hydroxylation, propane oxidative dehydrogenation) [1].

The preparation method of Fe-zeolites strongly influences the nature and distribution of the resulting iron species, which basically determines the catalyst performance. Extensive efforts have been dedicated to establishing reliable procedures for iron incorporation, including isomorphous substitution, ion exchange, and chemical vapor deposition (CVD) [2]. Introduction of iron in the zeolite matrix is typically followed by high-temperature calcination or steam treatment. The latter is crucial to yield active sites in isomorphously substituted zeolites by extraction of framework iron to extra-lattice positions [3]. The positive effect of steaming has also been reported for iron-containing zeolites prepared via CVD that were used in N_2O-mediated benzene hydroxylation [4]. Besides steaming, no other post-synthesis modification has been reported to improve the zeolite performance by changes in active site constitution and/or porous properties.

We have recently explored the opportunities of desilication (i.e., framework silicon extraction by post-treatment in alkaline medium) for controlled mesopore generation in zeolites with the ultimate aim of improving transport properties [5]. Tuneable mesoporosity has been achieved with preserved crystalline, microporous, and acidic properties. As a spin-off, mild alkaline leaching was successfully applied to defragment ZSM-5 zeolite crystals before the ion exchange with iron, leading to higher loadings as a result of shortened diffusional path lengths [6]. So far, desilication has not been applied to metal-containing zeolites.

Our strategy in the work reported here was to desilicate an iron-containing ZSM-5 zeolite, not only to create mesoporosity,

* Corresponding author. Fax: +31 15 278 44 52.
E-mail address: j.c.groen@tudelft.nl (J.C. Groen).

0021-9517/$ – see front matter
doi:10.1016/j.jcat.2006.07.001

but also to induce changes in the nature of the iron, potentially altering the zeolite catalytic performance. We applied the resulting materials in direct N_2O decomposition in view of its relevance in environmental catalysis. The recently commercialized EnviNO_x process by Uhde uses Fe-ZSM-5 for N_2O decomposition in nitric acid plants [7], and the achievement of catalysts operating at lower temperatures would be highly beneficial due to the limited tail gas temperature in two-thirds of the existing plants [8].

2. Experimental

2.1. Catalyst preparation

A commercial NH_4-ZSM-5 zeolite (PZ/2-40, Chemie Uetikon, nominal molar Si/Al ratio 25) was used in this study. Before further investigation, the sample was calcined in static air at 823 K for 5 h (this sample is denoted as Z25). Iron was introduced in the zeolite matrix by liquid-ion exchange at 353 K using iron(II) sulfate as a precursor following the procedure described by Pieterse et al. [9]. Subsequently, the sample was calcined in static air at 873 K for 2 h (Fe-Z25).

2.2. Post-synthesis modification treatments

Alkaline treatment of the calcined zeolites was performed in 0.2 M NaOH at 338 K for 30 min. After filtration and washing, the zeolites were dried at 373 K and calcined in static air at 823 K. The samples thus obtained are denoted with the suffix "at."

The alkaline-treated samples were converted into the H-form by two consecutive exchanges in 0.1 M NH_4NO_3 solution for 2 h. Subsequently the suspension was filtered and the solid was dried at 393 K. Final calcination of the zeolites was done in static air at 823 K for 5 h. The suffix "-ie" makes reference to the samples ion-exchanged in NH_4NO_3 solution.

2.3. Characterization

Chemical composition of the samples was determined by ICP-OES in a Perkin–Elmer Optima 4300DV. N_2 adsorption at 77 K was carried out in a Quantachrome Autosorb-6B apparatus. Samples were previously evacuated at 623 K for 16 h. Transmission electron microscopy was carried out in a Zeiss 10 CA electron microscope operated at 100 kV. The samples were mounted on a carbon-coated copper grid by placing a few droplets of the in chloroform suspended sample.

UV/vis diffuse reflectance (DR) spectra were recorded by a Cary 400 spectrometer (Varian) equipped with a diffuse reflectance accessory (Praying Mantis; Harrick) and a heatable reaction chamber connected to a gas-dosing system. The samples were diluted with α-Al_2O_3 to reduce light absorption. Spectra were recorded after the following treatments: 1 h O_2 flow at 823 K, 1 h 20% H_2/Ar flow at 823 K, 1 h 2% N_2O/He flow at 750 K (heating rate, 10 K min^{-1}; total flow rate, 20 cm^3 min^{-1}).

Mechanistic investigations of N_2O decomposition over the iron-containing zeolites were carried out in the Temporal Analysis of Products (TAP-2) reactor, a transient pulse technique with sub-millisecond time resolution [10]. The catalyst (25 mg; sieve fraction, 250–350 μm) was packed in the quartz microreactor (40 mm long, 6 mm i.d.) between two layers of quartz particles of the same sieve fraction. The catalyst was pretreated in flowing He (50 cm^3 STP min^{-1}) at 773 K and atmospheric pressure for 1 h. The pretreated sample was then exposed to vacuum (10^{-5} Pa) and the pulse experiments were subsequently performed. The direct N_2O decomposition was investigated at 823 K by pulsing N_2O:Ne = 1:1. The pulse size applied was 1×10^{15} molecules. The transient responses at the reactor outlet were monitored by quadrupole mass spectrometry at the following atomic mass units (AMU): 44 (N_2O), 32 (O_2), 30 (N_2O), 28 (N_2, N_2O), and 20 (Ne). In the experiments, 10 pulses were recorded and averaged for each AMU to improve the signal-to-noise ratio.

2.4. Activity

The activity of the various zeolites was tested in direct decomposition of N_2O. The experiments were carried out in a six-flow reactor system [11], using 40 mg of catalyst (sieve fraction, 125–250 μm) and a gas-hourly space velocity of 50,000 h^{-1}. The feed composition was 4.5 mbar N_2O in helium at a total pressure of 3 bar. N_2O conversion was measured with a gas chromatograph (Chrompack CP9001) equipped with a thermal conductivity detector and a Poraplot Q column.

3. Results and discussion

The parent zeolite (Z25) showed the typical microporous character without an appreciable contribution of mesoporosity, the latter being mostly a result of interparticle porosity in the aggregated crystals (Table 1). Liquid ion exchange led to an iron loading of 0.5 wt%, and, as expected, the porous properties of the ion-exchanged zeolite after calcination (Fe-Z25) were not altered. Upon alkaline treatment in 0.2 M NaOH, development of a distinct mesoporosity in the Fe-Z25at was demonstrated by N_2 adsorption. The mesopore surface area increased from 40 to 140 m^2 g^{-1}, ca. 25% lower than that in the alkaline-treated zeolite without iron (Z25at). Despite the significant mesoporosity development in Fe-Z25at, analysis of the filtrates revealed that the silicon leaching upon alkaline treatment of Fe-Z25 (650 mg Si L^{-1}) was ca. 5 times lower than in Z25at (3600 mg Si L^{-1}). This suggests that the presence of iron limits the formation of soluble silicates to a large extent and that formation of an iron silicate phase occurs (although XRD analyses have not evidenced the existence of such a phase). In addition, the micropore volume was lower in Fe-Z25at (0.11 cm^3 g^{-1}) than in Z25at (0.13 cm^3 g^{-1}), even after development of a lower degree of mesoporosity in the former. This is likely due to pore blockage by the suggested iron silicate phase in sample Fe-Z25at. Subsequent ion exchange of the alkaline-treated zeolite in NH_4NO_3 did not further alter the porous properties (Fe-Z25at-ie in Table 1).

The observed limited dissolution of silicon related to the presence of iron will likely affect the iron constitution in the

Table 1
Physico-chemical properties of the parent and Fe-ZSM-5 zeolites subjected to alkaline-treatment (at) in 0.2 M NaOH and ion exchange (ie) in 0.1 M NH_4NO_3

System	Molar Si/Al[a] (–)	Fe[a] (wt%)	$[Si]_{filtrate}$[a,b] ($mg\,L^{-1}$)	S_{BET}[c] ($m^2\,g^{-1}$)	S_{meso}[d] ($m^3\,g^{-1}$)	V_{micro}[d] ($m^3\,g^{-1}$)	TOF_{N_2O}[e] (s^{-1})	t_{max}[f] (s)
Z25	26	<0.02	–	410	35	0.16	–	–
Z25at	18	<0.02	3600	505	195	0.13	–	–
Z25at-ie	18	<0.02	–	500	190	0.13	–	–
Fe-Z25	26	0.5	–	410	40	0.16	6.5	0.27
Fe-Z25at	21	0.6	650	420	140	0.11	1.7	0.52
Fe-Z25at-ie	21	0.6	–	415	135	0.11	11.8	0.12

[a] ICP-OES.
[b] No iron was detected in the filtrate upon alkaline treatment or ion-exchange with NH_4NO_3.
[c] BET method.
[d] t-Plot method.
[e] Determined at $T = 765$ K.
[f] Time of the maximum in the oxygen transient response upon N_2O pulsing at 823 K in the TAP reactor.

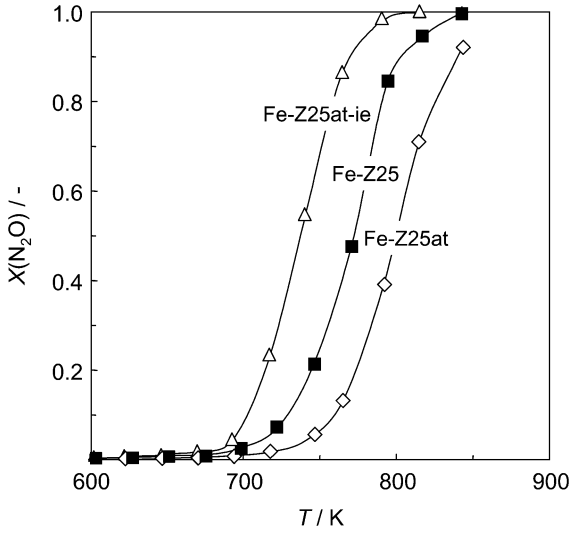

Fig. 1. N_2O conversion vs T over the iron-containing zeolites. Conditions: 4.5 mbar N_2O in He; $P = 3$ bar; gas-hourly space velocity = 50,000 h^{-1}.

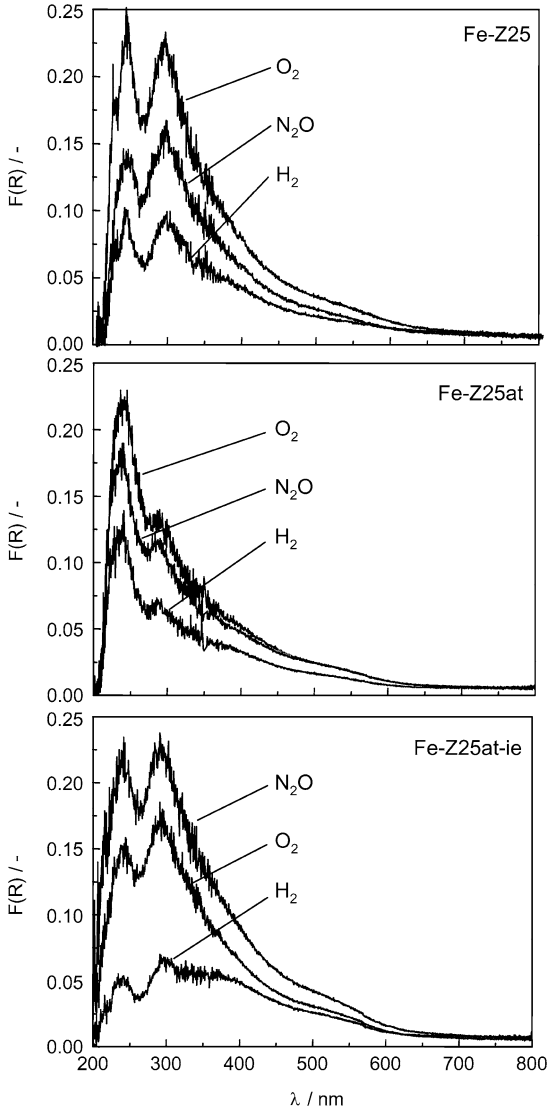

Fig. 2. UV/vis-DR spectra of the samples after oxidation in O_2 at 823 K, reduction in H_2 at 823 K, and reoxidation in N_2O at 750 K.

modified zeolites and the connected catalytic performance. Consequently, the activity of the various zeolites was assessed in direct N_2O decomposition. The calcined catalyst Fe-Z25 showed a significant N_2O conversion above 725 K and reached complete conversion at ca. 825 K. The alkaline-treated Fe-Z25at exhibited lower activity than the parent Fe-Z25; the overall activity profile is shifted 25 K to higher temperature. Surprisingly, the activity of Fe-Z25at-ie goes beyond that of Fe-Z25. The light-off temperature of Fe-Z25at-ie was significantly lower than that of Fe-Z25, presenting complete conversion at slightly below 800 K. Expressed in turnover frequencies (TOF), to correct for differences in iron content of the various systems (see Table 1), Fe-Z25at-ie is approximately twice as active than the parent catalyst Fe-Z25, and its TOF is 6 times higher than that of the alkaline-treated sample (Fe-Z25at).

The differences in catalytic performance shown in Fig. 1 are likely related to changes in iron speciation and/or connected redox properties upon the various treatments. To gain insight into the above, in situ UV/vis spectroscopic analyses were conducted. As depicted in Fig. 2, the spectra of all samples are characterized by broad, partially overlapping $Fe^{3+} \leftarrow O$ charge transfer bands. The assignment of these bands has been documented in detail elsewhere [12,13]. Briefly, a subband at around 240 nm arises from isolated Fe^{3+} sites in tetrahedral symme-

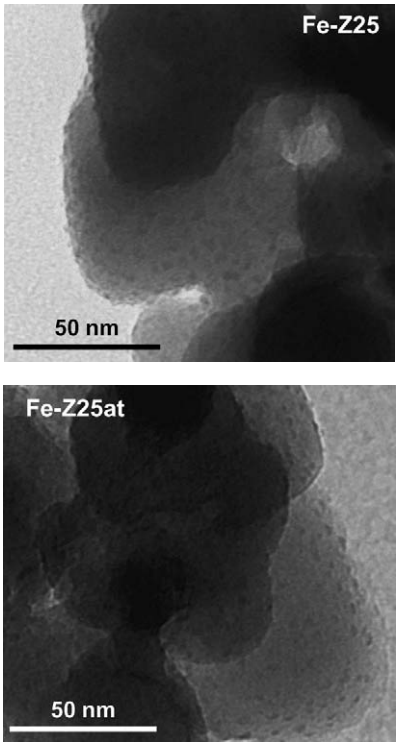

Fig. 3. TEM micrographs of Fe-Z25 and Fe-Z25at.

try, whereas single sites in higher coordination (5 or 6 oxygen ligands) give rise to an additional subband at around 290 nm. Bands at 300–400 nm are assigned to oligomeric clusters, and subbands at $\lambda > 400$ nm arise from large Fe_2O_3 particles. Comparing the spectra of preoxidized Fe-Z25 and Fe-Z25at reveals significant decreases in single octahedral Fe^{3+} and small oligonuclear clusters while the amounts of isolated tetrahedral Fe^{3+} and Fe_2O_3 particles remain practically unaffected. The latter observation agrees with TEM results (Fig. 3) showing iron oxide nanoparticles present to a similar extent before and after the alkaline treatment. This indicates that the alkaline treatment predominantly impacts the intrapore iron species. The intensity decrease of the octahedral Fe^{3+} band in Fe-Z25at is tentatively attributed to its reintegration in the ZSM-5 lattice and/or incorporation in the iron silicate phase as speculated above. This is also supported by the markedly higher resistance of Fe-Z25at toward reduction in H_2, which is characteristic of samples with Fe^{3+} in framework positions [13]. Moreover, a reference Fe-silicate phase prepared by treatment of goethite at 338 K in an alkaline sodium silicate solution showed no reduction in H_2 at 823 K, supporting our interpretation.

Subsequent treatment of Fe-Z25at in NH_4NO_3 solution (pH 5) altered the forms of iron from tetrahedral to octahedral and small oligonuclear sites, so that the original speciation observed in the original Fe-Z25 sample is apparently recovered. Similar to Fe-Z25, a large fraction of Fe^{3+} is sensitive to reduction by H_2, while iron oxide nanoparticles stay intact (Fig. 2). This suggests that nonreducible iron sites, probably residing in the iron silicate phase of sample Fe-Z25at, change nature upon treatment in the acidic NH_4NO_3 solution. Presumably, this occurs via intermediate reduction to Fe^{2+}. UV/vis experiments have revealed a significant increase in total absorbance after treatment of the as-received Fe-Z25at-ie sample in O_2, in contrast to Fe-Z25at (not shown). This indicates that in particular Fe-Z25at-ie contained a larger fraction of oxidizable Fe^{2+} species. Unlike sample Fe-Z25, the UV/vis intensity in sample Fe-Z25at-ie on N_2O treatment exceeds that after O_2 treatment. This strongly suggests that NH_4NO_3 treatment induces iron sites that can be oxidized by N_2O but not by O_2. Although bands associated with isolated Fe^{3+} ions and oligonuclear iron oxo species were present in the UV/vis spectra of both Fe-Z25 and Fe-Z25at-ie, and their relative areas were similar, the iron species in Fe-Z25at-ie exhibited a more pronounced redox activity on interaction with N_2O at 750 K. At this temperature, all three catalysts showed a measurable, significant difference in activity (see Fig. 1). Accordingly, the higher fraction of Fe^{2+} species in Fe-Z25at-ie and their relatively high degree of oxidation after N_2O treatment closely correlates with the higher activity of this catalyst in N_2O decomposition.

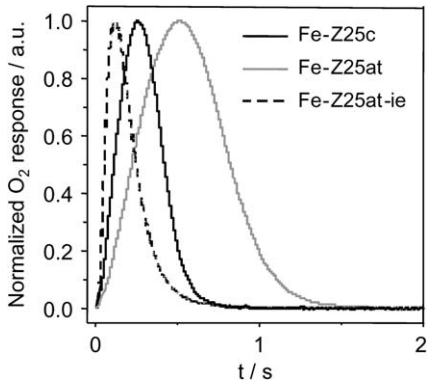

Fig. 4. Normalized transient responses of O_2 at 823 K upon single pulsing of $N_2O/Ne = 1/1$ over the differently treated iron-containing zeolites. Pulse size of $N_2O = 1 \times 10^{15}$ molecules.

Conclusive experimental evidence of the altered redox properties of the iron sites on the various treatments was gathered using the TAP-2 reactor. This transient pulse technique was previously successfully applied to rank deN_2O catalysts attending to the shape of the O_2 response upon N_2O pulsing [14]. This is conceivable, because O_2 desorption is the rate-determining step in this reaction [2a,14]. As can be seen in Fig. 4, the time required to obtain maximum response is longer with decreased steady-state activity of the catalysts, and the profiles broaden as well. Approximately 1.5 s was required for O_2 desorption in Fe-Z25at, compared with 0.5 s in Fe-Z25at-ie. This affirms that O_2 production during N_2O decomposition over Fe-Z25at-ie was easier than in Fe-Z25, particularly compared with the least active Fe-Z25at catalyst. Accordingly, alkaline treatment and successive ion exchange in NH_4NO_3 originated iron species with improved efficiency for O_2 desorption. Based on the similar UV/vis spectra of Fe-Z25 and Fe-Z25at-ie, it can be envisaged that the structure of the iron sites is alike in the two samples, but the distinctive redox behavior in the latter sample is determinative for achieving superior catalytic activity.

A similar trend in the metamorphosis of redox properties on the various post-treatments has been established over an iron-containing ZSM-5 zeolite of lower Si/Al ratio. As a result of the

much lower degree of silicon extraction and connected mesopore formation, due to the higher concentration of framework aluminium in this sample [5], the changes in redox behavior were less pronounced, but certainly significant.

In summary, alkaline treatment followed by ion exchange in NH_4NO_3 of Fe-ZSM-5 is an effective post-treatment that affects both the porosity of the zeolite and the nature of the iron species. Besides mesopore formation, it originates highly active sites and enhances the catalytic activity in direct N_2O decomposition. The improved catalytic performance has been correlated with changes in iron speciation leading to a higher concentration of Fe^{2+} species able to activate N_2O and improved desorption of O_2. To achieve such iron sites with unique redox behavior, it is essential to subject the iron-zeolite to the alkaline treatment, followed by ion exchange in an acidic NH_4NO_3 solution. These modified Fe-ZSM-5 catalysts also show promising potential in other catalytic conversions, such as selective oxidations of bulky hydrocarbons, where in addition to the altered redox properties, the created mesoporosity also may be beneficial. As controlled silicon extraction in alkaline medium, in view of framework silicon extraction and related mesoporosity development, has demonstrated its eligibility for other zeolite structures, such as beta [15] and ZSM-12 [16], the approach presented here should be translatable to other iron-containing zeolitic catalysts.

References

[1] (a) J. Pérez-Ramírez, F. Kapteijn, G. Mul, J.A. Moulijn, Chem. Commun. (2001) 693;
(b) H.-Y. Chen, T. Voskoboinikov, W.M.H. Sachtler, J. Catal. 180 (1998) 171;
(c) R.Q. Long, R.T. Yang, Chem. Commun. (2000) 1651;
(d) E.J.M. Hensen, Q. Zhu, R.A. van Santen, J. Catal. 233 (2005) 136;
(e) J. Pérez-Ramírez, E.V. Kondratenko, Chem. Commun. (2003) 2152.
[2] (a) G.D. Pirngruber, M. Lüchinger, P.K. Roy, A. Cecchetto, P. Smirniotis, J. Catal. 224 (2004) 429;
(b) K.S. Pillai, J. Jia, W.M.H. Sachtler, Appl. Catal. A 264 (2004) 133;
(c) J. Pérez-Ramírez, J.C. Groen, A. Brückner, M.S. Kumar, S. Bentrup, M.N. Debbagh, L.A. Villaescusa, J. Catal. 232 (2005) 318.
[3] J. Pérez-Ramírez, F. Kapteijn, J.C. Groen, A. Doménech, G. Mul, J.A. Moulijn, J. Catal. 214 (2003) 33.
[4] Q. Zhu, R.M. van Teeffelen, R.A. van Santen, E.J.M. Hensen, J. Catal. 221 (2004) 560.
[5] J.C. Groen, L.A.A. Peffer, J.A. Moulijn, J. Pérez-Ramírez, Chem. Eur. J. 11 (2005) 4983.
[6] I. Melián-Cabrera, S. Espinoza, J.C. Groen, B.v.d. Linden, F. Kapteijn, J.A. Moulijn, J. Catal. 238 (2006) 250.
[7] M. Schwefer, E. Szonn, T. Turek, WO 01/51181, 2001.
[8] J. Pérez-Ramírez, F. Kapteijn, K. Schöffel, J.A. Moulijn, Appl. Catal. B 44 (2003) 117.
[9] J.A.Z. Pieterse, S. Booneveld, R.W. van den Brink, Appl. Catal. B 51 (2004) 215.
[10] J.T. Gleaves, G.S. Yablonsky, P. Phanawadee, Y. Schuurman, Appl. Catal. A 160 (1997) 55.
[11] J. Pérez-Ramírez, R.J. Berger, G. Mul, F. Kapteijn, J.A. Moulijn, Catal. Today 60 (2000) 93.
[12] S. Bordiga, R. Buzzoni, F. Geobaldo, C. Lamberti, E. Giamello, A. Zecchina, G. Leofanti, G. Petrini, G. Tozzolo, G. Vlaic, J. Catal. 158 (1996) 486.
[13] J. Pérez-Ramírez, M.S. Kumar, A. Brückner, J. Catal. 223 (2004) 13.
[14] J. Pérez-Ramírez, J. Catal. 227 (2004) 512.
[15] J.C. Groen, L.A.A. Peffer, J.A. Moulijn, J. Pérez-Ramírez, Micropor. Mesopor. Mater. 69 (2004) 29.
[16] X. Wei, P. Smirniotis, presented at AIChE 2005 annual meeting, Cincinnati, October 2005.